

DERIVATIVE INFORMED NEURAL OPERATOR AN EFFICIENT FRAMEWORK FOR HIGH-DIMENSIONAL PARAMETRIC DERIVATIVE LEARNING*

THOMAS O'LEARY-ROSEBERRY[†], PENG CHEN^{*}, UMBERTO VILLA[‡], AND
OMAR GHATTAS[§]

Abstract.

Neural operators have gained significant attention recently due to their ability to approximate high-dimensional parametric maps between function spaces. At present, only parametric function approximation has been addressed in the neural operator literature. In this work we investigate incorporating parametric derivative information in neural operator training; this information can improve function approximations, additionally it can be used to improve the approximation of the derivative with respect to the parameter, which is often the key to scalable solution of high-dimensional outer-loop problems (e.g. Bayesian inverse problems). Parametric Jacobian information is formally intractable to incorporate due to its high-dimensionality, to address this concern we propose strategies based on reduced SVD, randomized sketching and the use of reduced basis surrogates. All of these strategies only require only $O(r)$ Jacobian actions to construct sample Jacobian data, and allow us to reduce the linear algebra and memory costs associated with the Jacobian training from the product of the input and output dimensions down to $O(r^2)$, where r is the dimensionality associated with the dimension reduction technique.

Numerical results for parametric PDE problems demonstrate that the addition of derivative information to the training problem can significantly improve the parametric map approximation, particularly given few data. When Jacobian actions are inexpensive compared to the parametric map, this information can be economically substituted for parametric map data. Additionally we show that Jacobian error approximations improve significantly with the introduction of Jacobian training data. This result opens the door to the use of derivative informed neural operators (DINOs) in outer-loop algorithms where they can amortize the additional training data cost via repeated evaluations.

Key words. Derivative learning, high-dimensional derivatives, neural operators, parametric surrogates, matrix-free methods, parametrized PDEs, derivative informed dimension reduction, adjoint-based sensitivity.

AMS subject classifications. 49M41, 65C20, 93E20, 93E35

1. Introduction. The so-called “neural operators” have gained significant attention in recent years due to their ability to approximate high-dimensional parametric maps between function spaces, and have become a major research topic in scientific machine learning (SciML) [6, 23, 27, 28, 29, 34, 33]. In this work we develop efficient algorithms for the construction and deployment of “derivative informed neural operators” (DINOs), which are faithful not only for the approximation of the parametric maps but also for their derivatives with respect to the input parameters. The inclusion of derivative information into the training of neural operators can improve the generalization accuracy of the underlying parametric map by enforcing that the neural operator respect the smoothness of the map at training data points, as in Her-

*This research partially supported by ARPA-E DIFFERENTIATE grant DE-AR0001208; NSF SI2-SSI grant ACI-1550593; DOE ASCR MMICC grant DE-SC0019303; and NSF DMS grant 2012453.

[†]Oden Institute for Computational Engineering & Sciences, The University of Texas at Austin, Austin, TX (tom.olearyroseberry@utexas.edu, peng@oden.utexas.edu).

[‡]McKelvey School of Engineering, Washington University in St. Louis, Saint Louis, MO (uvilla@wustl.edu).

[§]Oden Institute for Computational Engineering & Sciences, Jackson School of Geosciences, and Department of Mechanical Engineering, The University of Texas at Austin, Austin, TX (omar@oden.utexas.edu).

mite basis interpolation. Additionally the incorporation of this information improves the accuracy of the parametric derivative operator approximation, which increases the scope of their deployment to algorithmic contexts that require accurate derivative information. We use the term neural operator here in a broader context than the approximation of maps between function spaces and allow approximation of maps between any high-dimensional input and output. In this context, the derivatives are not directly approximated as matrices or tensors, but are instead accessed “matrix-free” through differentiation of the neural operator.

In the typical setting, a model is parameterized by parameters $m \in \mathbb{R}^{d_M}$ with probability distribution $m \sim \nu$, which are mapped to outputs $q(m) \in \mathbb{R}^{d_Q}$ through an implicit dependence on the solution of a model equation for the state variable $u \in \mathbb{R}^{d_U}$:

$$(1.1) \quad \underbrace{q(m) = q(u(m))}_{\text{Q.o.I. mapping}} \text{ where } u \text{ depends on } m \text{ through } \underbrace{R(u, m) = 0}_{\text{State model}},$$

where the dimensions $d_M, d_Q, d_U \in \mathbb{N}$ can be very high. These parametric maps usually arise via the discretization of partial differential equations, where m, u represent high-dimensional approximations of infinite dimensional field quantities. We consider quantity of interests (Q.o.I.s) that are generic functions of the state variable. Examples include parametric state maps (in the case that the full state is taken to be the Q.o.I.), as well as low-dimensional quantities such as sparse observations of the state, or other derived quantities.

The neural operator $f_w(m) = f(m, w) : \mathbb{R}^{d_M} \times \mathbb{R}^{d_W} \rightarrow \mathbb{R}^{d_Q}$ parametrized by both m and the weights variable $w \in \mathbb{R}^{d_W}$ is a fast-to-evaluate surrogate for the map $m \mapsto q$. The neural operator “learns” an approximation of the map by minimizing a data and/or physics informed loss function via nonlinear stochastic optimization with respect to w .

When the learning yields a sufficiently accurate approximation, these surrogates offer the possibility to accelerate and extend scientific inquiry and engineering problem solving by making tractable the solution of so-called “outer-loop” problems. Outer-loop problems, including forward uncertainty quantification, (Bayesian) inverse problems, optimal design and control, and optimal experimental design, often require repeated evaluations of the map $m \mapsto q$ as well as its derivatives. The scalability of most algorithms to solve outer-loop problems is limited by the costs of repeatedly computing the high-dimensional map for complex models whose solution is expensive to obtain. Outer-loop problems offer an ideal venue for the deployment of neural operators, since in this setting it is possible to amortize the offline costs of training data generation through repeated evaluations of the comparatively inexpensive surrogate.

The development of parametric surrogate modeling in SciML has focused on approximating the functional relationship $m \mapsto q$ over the distribution ν . Since the derivative approximation is not addressed directly in this context, it is generally unreasonable to expect derivatives $\nabla_m f_w$ to be reliable approximations of ∇q ¹. This shortcoming limits the deployment of the neural operators in outer-loop algorithms, since it restricts one to the use of “derivative-free” methods. The scalable solution of high-dimensional outer-loop problems often *requires* derivative information, since this information detects map sensitivities that can make problems effectively low-dimensional. This property has been observed and used in many outer-loop problems such as model

¹Consider for example the Weierstrass function which is everywhere continuous and nowhere differentiable.

reduction for sampling and deep learning [3, 4, 12, 34], optimization under uncertainty [2, 14, 16], Bayesian inverse problems [5, 8, 9, 10, 11, 13, 15, 17, 20, 22, 25, 42], and Bayesian optimal experimental design [1, 19, 37, 38, 39].

In this work we address the computational challenges associated with including derivative information in the neural operator training. We first formulate a derivative informed training problem over the parameter distribution ν , where the loss function includes a term for the neural operator approximation error of the (vector) output q and a term for the neural operator approximation error of the (matrix) derivative of the output ∇q . The major computational issues for constructing derivative informed neural operators arise due to the offline costs of generating Jacobian training data and the online computational and memory complexity of incorporating the derivative information into the optimization problem, since this formally requires evaluating the difference of two high-dimensional matrices of size $d_Q \times d_M$ at training points.

We propose to overcome these computational challenges by using compressed representation of the Jacobian ∇q . We target a broad class of problems for which the Jacobian at a point has low rank r ; in this case the costs of generating Jacobian training data requires $O(r)$ linear Jacobian matrix-vector products. For highly nonlinear high-dimensional maps this computation is asymptotically cheap in comparison to the evaluation of $m \mapsto q$. This dimension reduction additionally allows us to reduce the online computational and memory costs of including derivative information in the optimization problem from $O(d_Q d_M)$ to $O(r^2)$, where r is the intrinsic dimension of the derivative information.

We first begin by proposing the use of the reduced SVD of the Jacobian, which allows us to impose the dominant derivative curvature information in the r dimensional subspaces spanned by the left and right singular vectors of the Jacobian. This strategy is highly scalable, and improves the parametric map approximation by imposing dominant curvature conditions, but is itself insufficient to achieve accurate Jacobian approximations since it leaves the Jacobian nullspaces untouched. To overcome this issue we investigate random sketching techniques for computing the Jacobian error term, or in the case that the reduced SVD objective is used, to sketch complementary nullspace constraints. The proposed sketching based approach however incurs significant online computational costs in order to resolve the neural operators nullspace errors, and continually re-sketch the high-dimensional Jacobian data at every optimization epoch.

We ultimately propose the use of reduced basis ridge function neural operators, which only parametrize the nonlinear mapping $m \mapsto q$ in low-dimensional informed subspaces of the inputs and outputs. In this case, the model can only represent Jacobian information in the reduced subspaces of the inputs and outputs with dimensions $r_M \leq d_M, r_Q \leq d_Q$, which allows us to generate and impose Jacobian information in between only these two subspaces. This significantly reduces the online linear algebraic and memory costs to $O(r_Q r_M)$. In order to adequately resolve parametric Jacobian information, we advocate for the use of derivative informed projected neural networks (DIPNets)[34], which naturally incorporate dominant Jacobian information into their architectures and are thus well suited to learn the parametric derivative operator, in addition to the parametric map.

We investigate the effects of various different optimization formulations and neural network architectures on the accuracy of the approximation of the parametric map and its Jacobian by several numerical experiments. We consider parametric PDE problems where the parameters are given by the discretization of random coefficient fields that parametrize the PDE, and quantities of interest q given by sparse observation of the

PDE state variable. Numerical results demonstrate that the incorporation of derivative information in the neural operator training significantly improves the parametric map approximation, especially when training data are limited, as is often the case in SciML. Additionally numerical results demonstrate that these training formulations can result in significantly improved parametric derivative operator approximations. In particular, our numerical results imply that DIPNets perform better than generic networks in both parametric map and Jacobian approximation, showing that parametric surrogates with reliable derivative information can be constructed and trained in an efficient way by making use of derivative-revealed intrinsic low-dimensionality of the map.

1.1. Related works. The idea of incorporating derivative information into neural network training has been studied in [21] in a different setting, which did not address the computational challenges associated with high-dimensional maps, the use of derivative information extracted from the trained neural network, and experiments were limited to learning analytic functions or supplementing “synthetic derivatives” in order to improve the smoothness of the trained function. Our work differs from this work in scope and focuses on neural operators and efficient and scalable algorithms necessary for high-dimensional derivative training. We also motivate the need for derivative information in SciML outer-loop problems. A more recent paper [7] investigates using derivative information for constructing dimension reduced surrogates for scalar valued high-dimensional parametric maps via minimizing a gradient based objective function. The context of this paper is similar to ours; in our case we consider vector-valued high-dimensional maps with the focus on efficient algorithms and the approximation by neural operators.

There are many other papers on learning parametric PDE maps in a SciML context [6, 23, 27, 28, 29, 32, 34, 33, 35]. The algorithms advanced in this work are suitable to help any of these methods to learn high-dimensional derivative information and additionally improve approximations of high-dimensional parametric maps. This work concerns *parametric derivatives*, not to be confused with *spatial derivatives* which have been addressed in surrogate construction in various works [28, 40].

1.2. Contributions. Herein, we develop DINO, an efficient computational framework for encoding high-dimensional parametric derivative information into the training of neural operators to approximate high-dimensional parametric maps.

We first consider techniques based on reduced SVD to impose only the dominant curvature condition in the reduced SVD basis, reducing the computational costs from $O(d_Q d_M)$ to $O(r^2)$ where r is the rank of the Jacobian. We demonstrate that this computational cost can be reduced to $O(k^2)$ by making use of matrix subsampling techniques that randomly choose k rows and columns of the reduced Jacobian, and prove that this provides an asymptotically equivalent objective function in Proposition 2.2. The techniques based on reduced SVD are highly scalable and can improve approximation of the parametric map by imposing slope constraints in the directions where the map is changing the most, but alone are not sufficient to guarantee parametric Jacobian accuracy. To address this concern we consider techniques based on random matrix-sketching in order to impose the entire Jacobian information, or just the nullspace conditions if they are to be used in tandem with the reduced SVD techniques. Ultimately we do not favor this strategy due to slow asymptotics and online computational overhead during training.

We then investigate how reduced-basis surrogates can be used to provide a highly efficient framework for accurate parametric derivative learning. In regards to this

task, the fundamentally important feature of these surrogates is that they cannot represent Jacobian information that is orthogonal to their input and output reduced basis, as we prove in Proposition 2.4. This feature has two important consequences. First, it allows us to compute and impose full Jacobian information only in these reduced bases, again reducing the complexity from $O(d_Q d_M)$ to $O(r_Q r_M)$. Second, these surrogates can be architected to attempt to “build-out” the Jacobian nullspaces a priori, effectively using the architecture as a form of regularization for the derivative learning problem.

In three numerical experiments we demonstrate that the efficient incorporation of derivative information via DINO can improve the parametric map generalization when training data are limited. Additionally DINO leads to significantly improved approximation of parametric derivative operators over traditional parametric map regression. Among all the tested training strategies, the best overall strategy is to use the DIPNet network with full Jacobian information in the training. This strategy is scalable since the Jacobian information need only be represented in between the input and output reduced basis (which are often discretization independent), and accurate since the architecture is designed to resolve dominant Jacobian information, and nothing else.

At the time of writing we are unaware of any techniques for the efficient training of high-dimensional parametric surrogates on derivative information. We restrict ourselves to learning the first order parametric derivative (i.e. matrix free Jacobian), but the ideas are sufficiently general to be extended to higher derivative tensor actions. The approach we propose relies on the compressibility of high dimensional Jacobian information; DINO may not be suitable for problems that have high-dimensional Jacobian information across parameter space, an example of this may be full parametric state estimation for non-dissipative hyperbolic PDE problems.

2. Derivative informed neural operator. Let $H_\nu^1(\mathbb{R}^{d_M}; \mathbb{R}^{d_Q})$ denote a (discrete Bochner) space for the map $q : \mathbb{R}^{d_M} \rightarrow \mathbb{R}^{d_Q}$ with the norm given by

$$(2.1) \quad \begin{aligned} \|q\|_{H_\nu^1(\mathbb{R}^{d_M}; \mathbb{R}^{d_Q})}^2 &= \mathbb{E}_\nu \left[\|q\|_{H^1(\mathbb{R}^{d_Q})}^2 \right] \\ &= \int_{\mathbb{R}^{d_M}} \left(\|q(m)\|_{\ell^2(\mathbb{R}^{d_Q})}^2 + \|\nabla q(m)\|_{F(\mathbb{R}^{d_Q \times d_M})}^2 \right) d\nu(m), \end{aligned}$$

where $\|q(m)\|_{\ell^2(\mathbb{R}^{d_Q})}$ is the Euclidean norm of the output q evaluated at m and $\|\nabla q(m)\|_{F(\mathbb{R}^{d_Q \times d_M})}$ is the Frobenius norm of the Jacobian ∇q evaluated at m , which we refer to as the H^1 *semi-norm* in the rest of the paper. The derivative informed neural operator $f_w = f(\cdot, w) : \mathbb{R}^{d_M} \times \mathbb{R}^{d_W} \rightarrow \mathbb{R}^{d_Q}$ is a parametric neural network surrogate parametrized by weights $w \in \mathbb{R}^{d_W}$, which is constructed by attempting to solve the following expected risk minimization problem:

$$(2.2) \quad \min_w \frac{1}{2} \mathbb{E}_\nu \left[\|q - f_w\|_{H^1(\mathbb{R}^{d_Q})}^2 \right].$$

Note that each evaluation of the output q requires solution of the state equation (1.1), which is often very expensive, and makes it prohibitively expensive to accurately approximate the integral with respect to ν in (2.2). This issue is addressed via Monte Carlo sample average approximation of (2.2): given a finite (affordably small) number of training samples $\{(m_i, q(m_i), \nabla q(m_i)) | m_i \sim \nu\}_{i=1}^N$ we can bypass direct integration

by instead formulating the following empirical risk minimization:

$$(2.3) \quad \min_w \frac{1}{2N} \sum_{i=1}^N \|q(m_i) - f_w(m_i)\|_{H^1(\mathbb{R}^{d_Q})}^2.$$

The empirical risk objective function in (2.3) can be differentiated with respect to the weights w by automatic differentiation, which allows for the neural operator to be trained via derivative-based nonlinear stochastic optimization methods. The critical computational challenge is to compute the Jacobian term

$$(2.4) \quad \|\nabla q(m) - \nabla f_w(m)\|_{F(\mathbb{R}^{d_Q \times d_M})}^2,$$

which is the focus of this work. Formally the offline costs of computing full Jacobian training data are expensive per datum, and the online memory and linear algebra costs of evaluating the Frobenius norm of the Jacobian misfit incurs $O(d_Q d_M)$ complexity. This makes the derivative training task formally intractable when d_Q and d_M are large.

In practice, however, the Jacobian matrices are often low rank because of (1) the correlation in both the input parameters and the output QoIs, and (2) the smoothness of the map, which can be efficiently approximated by low rank matrices with rank $r \ll d_Q, d_M$, or $r = O(d_Q) \ll d_M$ as is the case in inverse problems where observations are sparse. This low-rank property of the Jacobian matrix has been observed and used in many inverse problems [5, 8, 9, 11, 10, 13, 15, 17, 20, 22, 25, 42]. When this is the case, Jacobian training data can be computed for $O(r)$ linear Jacobian matrix-vector products at each data point, e.g. using randomized SVD [?], and the online computational and memory costs of training can be made to scale with $O(r^2)$ instead of $O(d_Q d_M)$. In this work, we discuss strategies to achieve this complexity in training, by making use of different dimension reduction techniques.

2.1. Approximation of H^1 semi-norm via reduced SVD. At a parameter sample we can decompose the Jacobian into its rank r reduced SVD and the contributions of the orthogonal complements:

$$(2.5a) \quad \nabla q = U_r \Sigma_r V_r^T + U_r^\perp 0(V_r^\perp)^T.$$

All of the information about the Jacobian is contained in the reduced SVD, since the orthogonal complements to the dominant left and right singular vectors are accessible via orthogonal projectors

$$(2.5b) \quad \text{span}(U_r^\perp) = \text{span}(I_{d_Q} - U_r U_r^T),$$

$$(2.5c) \quad \text{span}(V_r^\perp) = \text{span}(I_{d_M} - V_r V_r^T).$$

A first idea that we consider is to decompose the Jacobian information into the reduced SVD basis, thus separating local dominant curvature conditions from nullspace conditions. In this approach, the goal is to get the derivatives of the neural operator to match in the dominant subspaces defined by the reduced SVD, which can improve the parametric map approximation by enforcing smooth interpolation of the map between training data. Additionally this approach can be used to achieve accurate approximations of the full Jacobian, if it is used in tandem with a efficient approach to penalize learning curvature in the nullspaces of the Jacobian. We start with a proposition for the decomposition of the Jacobian error into low-dimensional curvature conditions and complementary nullspace conditions.

PROPOSITION 2.1. *Decomposing the Jacobian error via reduced SVD for ∇q . At every parameter sample there hold*

$$(2.6a) \quad \Sigma_r - U_r^T \nabla_m f_w V_r = 0 \in \mathbb{R}^{r \times r},$$

$$(2.6b) \quad (I_{d_Q} - U_r U_r^T) \nabla_m f_w (I_{d_M} - V_r V_r^T) = 0 \in \mathbb{R}^{d_Q \times d_M},$$

$$(2.6c) \quad (I_{d_Q} - U_r U_r^T) \nabla_m f_w V_r = 0 \in \mathbb{R}^{d_Q \times d_M},$$

$$(2.6d) \quad U_r^T \nabla_m f_w (I_{d_M} - V_r V_r^T) = 0 \in \mathbb{R}^{d_Q \times d_M},$$

if and only if

$$(2.6e) \quad \nabla q = \nabla_m f_w.$$

Proof. We begin with a simple auxiliary result. Let $A \in \mathbb{R}^{m \times n}$ be an arbitrary matrix and $Q_r \in \mathbb{R}^{n \times r}$ be orthonormal, (i.e. $Q_r^T Q_r = I_r \in \mathbb{R}^{r \times r}$), then we have

(2.7)

$$\|AQ_r Q_r^T\|_{F(\mathbb{R}^{m \times n})} = \sqrt{\text{tr}(AQ_r Q_r^T Q_r Q_r^T A)} = \sqrt{\text{tr}(AQ_r Q_r^T A^T)} = \|AQ_r\|_{F(\mathbb{R}^{m \times r})}.$$

By repeated use of the orthogonal decomposition identity we have

$$\begin{aligned} \|\nabla q - \nabla_m f_w\|_{F(\mathbb{R}^{d_Q \times d_M})} &= \|U_r U_r^T (\nabla q - \nabla_m f_w) V_r V_r^T\|_{F(\mathbb{R}^{d_Q \times d_M})} \\ &\quad + \|(I_{d_Q} - U_r U_r^T) (\nabla q - \nabla_m f_w) (I_{d_M} - V_r V_r^T)\|_{F(\mathbb{R}^{d_Q \times d_M})} \\ &\quad + \|(I_{d_Q} - U_r U_r^T) (\nabla q - \nabla_m f_w) V_r V_r^T\|_{F(\mathbb{R}^{d_Q \times d_M})} \\ (2.8) \quad &\quad + \|U_r U_r^T (\nabla q - \nabla_m f_w) (I_{d_M} - V_r V_r^T)\|_{F(\mathbb{R}^{d_Q \times d_M})}. \end{aligned}$$

Note that ∇q disappears in each term involving the left application of $(I_{d_Q} - U_r U_r^T)$ or the right application of $(I_{d_M} - V_r V_r^T)$, by the definition of the reduced SVD. Applying this result with multiple applications of (2.7) we get the following:

$$\begin{aligned} \|\nabla q - \nabla_m f_w\|_{F(\mathbb{R}^{d_Q \times d_M})} &= \|\Sigma_r - U_r^T \nabla_m f_w V_r\|_{F(\mathbb{R}^{r \times r})} \\ &\quad + \|(I_{d_Q} - U_r U_r^T) \nabla_m f_w (I_{d_M} - V_r V_r^T)\|_{F(\mathbb{R}^{d_Q \times d_M})} \\ &\quad + \|(I_{d_Q} - U_r U_r^T) \nabla_m f_w V_r\|_{F(\mathbb{R}^{d_Q \times r})} \\ (2.9) \quad &\quad + \|U_r^T \nabla_m f_w (I_{d_M} - V_r V_r^T)\|_{F(\mathbb{R}^{r \times d_M})}. \quad \square \end{aligned}$$

Substituting the assumptions of the proposition sets the right hand side to zero, and the result follows.

Proposition 2.1 establishes that dominant curvature conditions can be imposed at sample points for only $O(r^2)$ work. For certain problems however, depending on how large r is, penalizing a Frobenius norm in $\mathbb{R}^{r \times r}$ may still be untenable. The reasons being that automatic differentiation requires significant memory and operational overhead, while stochastic optimization requires that additional memory be allocated for additional arrays used in evaluating finite sum gradients and Hessians used in the training of the neural operator. We propose to further ease this computational burden by randomly subsampling left and right singular vectors at each epoch of training. In the following proposition we discuss the approximation of the true Frobenius curvature condition by row and column subsampling.

PROPOSITION 2.2. *Approximation of submatrix truncated SVD H^1 semi-norm in expectation*

Let κ be a distribution of k indices subsampled from $1, \dots, r$ with uniform probability. Denote samples of these indices by $[\hat{k}], [\tilde{k}]$, and the subsampled matrices by $U_{[\hat{k}]} \in \mathbb{R}^{d_Q \times k}, V_{[\tilde{k}]} \in \mathbb{R}^{d_M \times k}$, etc.. When k columns of U_r and V_r are subsampled independently then

$$(2.10) \quad \mathbb{E}_{[\hat{k}], [\tilde{k}] \sim \kappa} \left[\|\Sigma_{[\hat{k}], [\tilde{k}]} - U_{[\hat{k}]}^T \nabla_m f_w V_{[\tilde{k}]} \|_{F(\mathbb{R}^{k \times k})}^2 \right] = \frac{k^2}{r^2} \|\Sigma_r - U_r^T \nabla_m f_w V_r \|_{F(\mathbb{R}^{r \times r})}^2.$$

Here $\Sigma_{[\hat{k}], [\tilde{k}]} = U_{[\hat{k}]}^T U_r \Sigma_r V_r^T V_{[\tilde{k}]}.$ When the same k columns are subsampled for both U_r and V_r , then

$$(2.11) \quad \begin{aligned} \mathbb{E}_{[\hat{k}] \sim \kappa} \left[\|\Sigma_{[\hat{k}], [\hat{k}]} - U_{[\hat{k}]}^T \nabla_m f_w V_{[\hat{k}]} \|_{F(\mathbb{R}^{k \times k})}^2 \right] &= \frac{k}{r} \|diag(\Sigma_r - U_r^T \nabla_m f_w V_r)\|_{F(\mathbb{R}^{r \times r})}^2 \\ &+ \frac{k(k-1)}{r(r-1)} \|offdiag(\Sigma_r - U_r^T \nabla_m f_w V_r)\|_{F(\mathbb{R}^{r \times r})}^2. \end{aligned}$$

Proof. Let $B = U_r \Sigma_r V_r^T - \nabla_m f_w.$ We begin with the case of independent left and right column samples. Let $\chi_{i \in [\tilde{k}]}$ denote the indicator function that the index i is in the index subset $[\tilde{k}]$, which implies $\mathbb{E}_{[\tilde{k}] \sim \kappa} [\chi_{i \in [\tilde{k}]}] = \frac{k}{r}$ for any $i = 1, \dots, r.$ We have then that

$$(2.12) \quad \|U_{[\tilde{k}]}^T B V_{[\tilde{k}]} \|_{F(k \times k)}^2 = \sum_{i=1}^r \sum_{j=1}^r \chi_{i \in [\tilde{k}]} \chi_{j \in [\tilde{k}]} (U_r^T B V_r)_{ij}^2,$$

where we used $\chi_{i \in [\tilde{k}]} = \chi_{i \in [\tilde{k}]}^2.$ Taking expectation we have

$$(2.13) \quad \begin{aligned} \mathbb{E}_{[\hat{k}], [\tilde{k}] \sim \kappa} \left[\|U_{[\tilde{k}]}^T B V_{[\tilde{k}]} \|_{F(k \times k)}^2 \right] &= \mathbb{E}_{[\hat{k}], [\tilde{k}] \sim \kappa} \left[\sum_{i=1}^r \sum_{j=1}^r \chi_{i \in [\tilde{k}]} \chi_{j \in [\tilde{k}]} (U_r^T B V_r)_{ij}^2 \right] \\ &= \sum_{i=1}^r \sum_{j=1}^r \mathbb{E}_{[\hat{k}], [\tilde{k}] \sim \kappa} \left[\chi_{i \in [\tilde{k}]} \chi_{j \in [\tilde{k}]} \right] (U_r^T B V_r)_{ij}^2 = \frac{k^2}{r^2} \sum_{i=1}^r \sum_{j=1}^r (U_r^T B V_r)_{ij}^2. \end{aligned}$$

For the case that the left and right samples are the same we have

$$(2.14) \quad \begin{aligned} \|U_{[\hat{k}]}^T B V_{[\hat{k}]} \|_{F(k \times k)}^2 &= \sum_{i=1}^r \sum_{j=1}^r \chi_{i \in [\hat{k}]} \chi_{j \in [\hat{k}]} (U_r^T B V_r)_{ij}^2 \\ &= \sum_{i=1}^r \chi_{i \in [\hat{k}]} (U_r^T B V_r)_{ii}^2 + \sum_{i=1}^r \sum_{i \neq j=1}^r \chi_{i \in [\hat{k}]} \chi_{j \in [\hat{k}] \setminus \{i\}} (U_r^T B V_r)_{ij}^2. \end{aligned}$$

Taking expectation we have

$$\mathbb{E}_{[\tilde{k}] \sim \kappa} \left[\|U_{[\tilde{k}]}^T B V_{[\tilde{k}]} \|_{F(k \times k)}^2 \right] = \frac{k}{r} \sum_{i=1}^r (U_r^T B V_r)_{ii}^2 + \frac{k}{r} \frac{(k-1)}{(r-1)} \sum_{i=1}^r \sum_{i \neq j=1}^r (U_r^T B V_r)_{ij}^2. \quad \square$$

This proposition establishes that in either case using independent or dependent samples for rows and columns, the subsampled approximation of the Frobenius norm serves as an asymptotically equivalent optimization objective function, which can be scalably incorporated into training independent of how large r is. In the case that the same samples are used for both the rows and columns, the effects of the diagonals of the matrix are over-emphasized. Since Σ_r is by definition a diagonal matrix, this can be a beneficial property since it guarantees that there will always be k nonzero curvature conditions that are imposed at each sample. In the case that independent samples are used it is possible that only off diagonal elements of Σ_r will show up in the loss function, which in our experience can make the optimization problem harder. Proposition 2.2 demonstrates the curvature conditions can be imposed in a memory efficient way, even when r is large.

The imposition of low-dimensional curvature conditions is generic and can be imposed in a matrix-free way. The low-dimensional curvature information can be extracted from generic differentiable surrogates / neural operators via use of automatic differentiation; a schematic for this is shown in Figure 1.

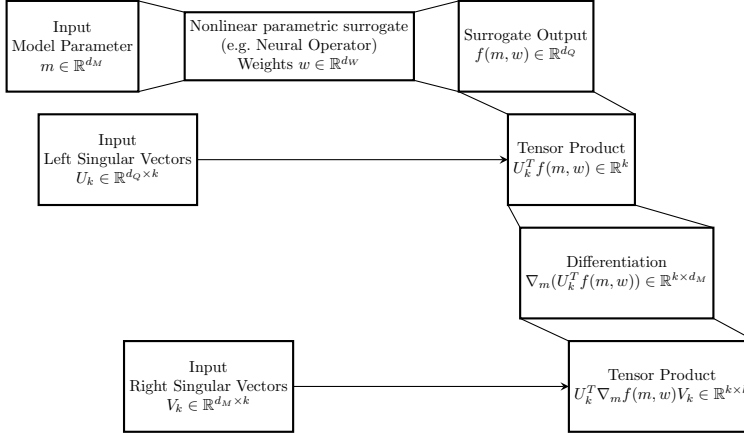


Fig. 1: Schematic operation chart for extracting low-dimensional sensitivities from neural operators. All operations can be vectorized over an additional data dimension.

Numerical results in Section 3 demonstrate that the inclusion of the reduced Jacobian information, particularly with matrix subsampling improve the parametric map approximation. Similar to Hermite interpolation methods, we suppose that the inclusion of dominant curvature information at training data points leads to more accurate interpolation in between training data points in the directions that the parametric map is changing the most. This makes the strategy desirable in contexts where one cares about the most about more accurate parametric map approximations. Imposing the reduced Jacobian curvature constraints alone does not guarantee accurate Jacobian; in order to achieve accurate parametric Jacobian the nullspace conditions still need to be addressed directly via the optimization formulation, or indirectly through the design of the architecture. We propose strategies for these tasks in the following sections.

2.2. Random sketching of Jacobian Information. Both the full Jacobian error condition $\nabla q - \nabla f_w = 0$, as well as the nullspace conditions (2.6b, 2.6c, 2.6d)

formally require $O(d_Q d_M)$ computation for their evaluation. In this section we discuss strategies for reducing this computational burden via the use of random matrix sketching. All three of these constraints can be stated generically as $A = 0$. Via randomized matrix sketching, we can approximate the constraint error $\|A\|_{F(\mathbb{R}^{d_Q \times d_M})}$ by the use of random rank r left and right sketches, as $\|Q_{\text{left}}^T A Q_{\text{right}}\|_{F(\mathbb{R}^{r \times r})}$, thus reducing the computational complexity from $O(d_Q d_M)$ to $O(r^2)$, where r here is the dimension of the sketching. By resampling different random matrices at different optimization epochs, the constraints are imposed *in expectation* with respect to the underlying distribution of random matrices.

PROPOSITION 2.3. *Approximation of matrix equation constraints via sketching*
Given (e.g. Gaussian) distributions of random orthonormal matrices $\mathbb{R}^{d_Q \times r} \ni Q_{\text{left}} \sim \rho_{\text{left}}$, and $\mathbb{R}^{d_M \times r} \ni Q_{\text{right}} \sim \rho_{\text{right}}$, the approximation of the full matrix constraint equation by the sketching has the following bound in expectation with respect to the sampling distributions:

$$(2.15) \quad \begin{aligned} \|A\|_{F(\mathbb{R}^{d_Q \times d_M})} &\leq \mathbb{E}_{\rho_{\text{left}}, \rho_{\text{right}}} [\|Q_{\text{left}}^T A Q_{\text{right}}\|_{F(\mathbb{R}^{r \times r})}] \\ &\quad + C(\rho_{\text{left}}, \rho_{\text{right}}, d_M, d_Q) \sum_{j=r+1}^{\min(d_M, d_Q)} \sigma_j(A), \end{aligned}$$

where $\sigma_j(A)$ is the j^{th} singular value of A .

Proof. We can sample random orthonormal matrices by first sampling a random matrix from an existing distribution, $\Omega \sim \rho$ and then performing a reduced QR decomposition to compute an orthonormal basis Q . By applying Theorem 15.3 in [31] to the left of A ,

$$(2.16) \quad \mathbb{E}_{\rho_{\text{left}}} [\|A - Q_{\text{left}} Q_{\text{left}}^T A\|_{F(\mathbb{R}^{d_Q \times d_M})}] \leq C_1(\rho_{\text{left}}, d_M, d_Q) \sum_{j=s+1}^{\min(d_M, d_Q)} \sigma_j(A),$$

and then a second time to the transpose of $Q_{\text{left}} Q_{\text{left}}^T A$, we obtain

$$(2.17) \quad \begin{aligned} &\mathbb{E}_{\rho_{\text{left}}, \rho_{\text{right}}} [\|Q_{\text{left}} Q_{\text{left}}^T A - Q_{\text{left}} Q_{\text{left}}^T A Q_{\text{right}} Q_{\text{right}}^T\|_{F(\mathbb{R}^{d_Q \times d_M})}] \\ &\leq C_2(d_M, d_Q) \sum_{j=s+1}^{\min(d_M, d_Q)} \sigma_j(Q_{\text{left}} Q_{\text{left}}^T A) \leq C_2(d_M, d_Q) \sum_{j=s+1}^{\min(d_M, d_Q)} \sigma_j(A), \end{aligned}$$

the two terms can be combined via the triangle inequality, which yields the following bound via another use of the triangle inequality,

$$(2.18) \quad \begin{aligned} \|A\|_{F(\mathbb{R}^{d_Q \times d_M})} &\leq \mathbb{E}_{\rho_{\text{left}}, \rho_{\text{right}}} [\|Q_{\text{left}} Q_{\text{left}}^T A Q_{\text{right}} Q_{\text{right}}^T\|_{F(\mathbb{R}^{d_Q \times d_M})}] \\ &\quad + C(\rho_{\text{left}}, \rho_{\text{right}}, d_M, d_Q) \sum_{j=r+1}^{\min(d_M, d_Q)} \sigma_j(A), \end{aligned}$$

here the constants C_1, C_2 are combined into one constant C . By making use of an auxiliary result in Proposition 2.1 we have that $\|Q_{\text{left}} Q_{\text{left}}^T A Q_{\text{right}} Q_{\text{right}}^T\|_{F(\mathbb{R}^{d_Q \times d_M})} = \|Q_{\text{left}}^T A Q_{\text{right}}\|_{F(\mathbb{R}^{r \times r})}$, which yields the result. \square

If the trailing singular values are small, and we can minimize the sketched constraint in expectation, then this inequality demonstrates that the constraint $A = 0$ will also be satisfied. This however is a difficult task in practice since the singular value decay of A depends not only on ∇q , but also on ∇f_w . If f_w has significant curvature in the nullspaces of ∇q , then large sketching dimension r may be required to adequately penalize these terms. Additionally there is a significant amount of additional computational overhead to this sketching approach, since at each epoch, new sketching matrices must be computed, along with the sketching Jacobian information in the online training procedure. The benefit of this approach is that it is generic; it can be used to impose the full Jacobian constraints without making any assumptions on the underlying structure of the architecture, or it can be used in tandem with the reduced curvature approach delineated in Section 2.1 by sketching the nullspace constraints in a complementary low-dimensional subspace.

In what follows we propose that by making assumptions on the architecture of the neural operator we can propose a much better overall strategy. By using reduced basis architectures we can scalably handle both the full Jacobian information, or the nullspace conditions due to properties of these neural operators.

2.3. Reduced Basis Derivative Learning. Consider an input-output ridge function surrogate

$$(2.19) \quad f^r(m, w) = \mathbf{U}_{\mathbf{r}_Q} \phi_r(\mathbf{V}_{\mathbf{r}_M}^T m, w) + b,$$

where ϕ_r now parametrizes a reduced dimensional nonlinear operator between the two reduced bases [6, 33, 34], where $\mathbf{U}_{\mathbf{r}_Q} \in \mathbb{R}^{d_Q \times \mathbf{r}_Q}$ and $\mathbf{V}_{\mathbf{r}_M} \in \mathbb{R}^{d_M \times \mathbf{r}_M}$ are adequate reduced bases for the inputs and outputs for the map $m \mapsto q$ and its derivative. A property of these functions is that their Jacobian with respect to m cannot represent information in the orthogonal complements of the input and output reduced bases.

PROPOSITION 2.4. *Orthogonality Conditions for Ridge Function Jacobian Without loss of generality take $\mathbf{r} = \mathbf{r}_Q = \mathbf{r}_M$.*

1. *If $X_{r_i} \perp \mathbf{V}_r$, then $\nabla_m f_w^r X_{r_i} = 0$.*
2. *If $Y_{r_i} \perp \mathbf{U}_r$, then $Y_{r_i}^T \nabla_m f_w^r = 0$.*

Proof. Consider an arbitrary column $x_j \in \text{col}(X_{r_i})$ indexed by j , and an arbitrary component of the output $(f_w^r)_k$ indexed by k . This represents the j, k entry in the matrix $\nabla_m f_w^r X_{r_i}$. In the limit definition this entry is

$$(2.20) \quad \nabla_m (f_w^r)_k x_j = \lim_{h \rightarrow 0} \frac{(f^r(m_i + hx_j, w)_k - f^r(m_i, w)_k)}{h}.$$

Due to the orthogonality condition

$$(2.21) \quad \mathbf{V}_r(m_i + hx_j) = \mathbf{V}_r m_i + h \mathbf{V}_r \xrightarrow{0} x_j = \mathbf{V}_r m_i,$$

and thus $(f^r(m_i + hx_j, w)_k - f^r(m_i, w)_k) = 0$, so the directional derivative is zero. This concludes the proof of the first proposition.

For the second proposition consider the j, k entry of $Y_{r_i}^T \nabla_m f_w^r$. This corresponds to the quantity

$$(2.22) \quad y_j^T \frac{\partial f_w^r}{\partial m^{(k)}},$$

where y_j is the j^{th} column of Y_{r_i} and $m^{(k)}$ is the k^{th} Cartesian basis vector in \mathbb{R}^{d_M} . In the limit definition we have

$$(2.23) \quad \begin{aligned} \lim_{h \rightarrow 0} \frac{1}{h} y_j^T \left[f^r(m_i + hm^{(k)}, w) - f^r(m_i, w) \right] = \\ \lim_{h \rightarrow 0} \frac{1}{h} y_j^T \mathbf{U}_r^T \left[\phi_r(\mathbf{V}_r(m_i + hm^{(k)}), w) - \phi_r(\mathbf{V}_r m_i, w) \right] = 0. \end{aligned} \quad \square$$

We emphasize two consequences of this proposition. First, if the important Jacobian information is well resolved between the reduced bases, i.e. $\mathbb{E}_\nu[\|\nabla q - \mathbf{U}_r \mathbf{U}_r^T \nabla q \mathbf{V}_r \mathbf{V}_r^T\|_{F(\mathbb{R}^{d_Q \times d_M})}] < \epsilon$ for $0 < \epsilon$ sufficiently small, then one can still use the total Jacobian information for $O(\mathbf{r}^2)$ compute. In this case, the cost of the Jacobian training data construction is reduced since the surrogate can only represent $\mathbf{U}_r^T \nabla q \mathbf{V}_r$, which can be computed at sample points for significantly reduced cost and only need be imposed in training as $\|\mathbf{U}_r^T \nabla q \mathbf{V}_r - \mathbf{U}_r^T \nabla f_w \mathbf{V}_r\|_{F(\mathbb{R}^{r \times r})}$. Second, if Jacobian nullspaces are precluded from \mathbf{U}_r and \mathbf{V}_r , then one can use the reduced SVD objective delineated in section 2.1 and have the architecture approximately satisfy the nullspace constraints, passively.

In either case, the key issue is constructing reduced bases \mathbf{U}_r and \mathbf{V}_r that adequately resolve the dominant left and right nullspaces of the parametric Jacobian *in expectation*. In the second case it is specifically important to attempt to preclude the Jacobian nullspaces. For this task, we consider two bases that attempt to resolve these bases in expectation. The right singular vectors of the Jacobian (weighted by the square of the singular values) are captured by the “active subspace” basis (AS), i.e. the dominant eigenvectors of

$$(2.24) \quad \mathbb{E}_\nu[\nabla q^T \nabla q] \in \mathbb{R}^{d_M \times d_M},$$

in expectation. The AS basis is a powerful derivative based dimension reduction technique that resolves the dominant sensitivity information of a parametric map in expectation. It has been useful in dimension reduction techniques and surrogate modeling [18, 34, 41]. A related basis can be constructed to capture the dominant information contained in the left singular vectors of the Jacobian (again weighted by the square of the singular values):

$$(2.25) \quad \mathbb{E}_\nu[\nabla q \nabla q^T] \in \mathbb{R}^{d_Q \times d_Q}.$$

We refer to this basis as the derivative outer product basis. Approximation bounds for ridge function approximations are well known for the active subspace basis [41], bounds for the approximation of the Jacobian in the derivative outer product basis are outside of the scope of this work. We conjecture that the approximation bound is analogous to that by proper orthogonal decomposition [30] for the output, but here for the first order derivative of the output.

Reduced basis neural networks based on active subspace are referred to as derivative informed projected neural networks (DIPNets)[34], and given limited training data can achieve high accuracy in approximating parametric functions by focusing on the most sensitive directions of parameter space. These networks are well suited to derivative approximation based on the prior discussion. The combination of DIPNets with the efficient approximation of the Jacobian in the combined reduced bases creates an accurate and scalable approach to approximating parametric maps and derivatives, as demonstrated by numerical results in the next section.

3. Numerical Experiments. In this section we demonstrate the accuracy and efficiency of four different optimization formulations for three different network architectures to approximation parametric maps with PDE constraints, all for varying availability of training data. In general our numerical results show that Jacobian information has positive effects on the L^2 generalization accuracy of the parametric map approximation and resulted in more accurate approximations of derivatives. Additionally the use of derivative informed reduced basis networks led to efficient strategies for learning accurate parametric map and Jacobian approximations simultaneously. The code for these numerical results can be found at <https://github.com/tomoleary/dino>.

3.1. Definition of Parametric PDE Maps.

We consider PDE problems where the mapping $m \mapsto q$ represents a mapping from a random coefficient field that parametrizes the PDE to the observable of the PDE state variable at points inside of the domain of the PDE. We use a centered Gaussian distribution $\nu = \mathcal{N}(0, \mathcal{C})$ for the random field with a trace-class Matérn covariance $\mathcal{C} = \mathcal{A}^{-2}$, where

$$(3.1) \quad \mathcal{A} = (\delta I - \gamma \Delta),$$

defined in physical domain Ω and imposed with homogeneous Neumann boundary condition. The correlation structure is parametrized by $\delta, \gamma > 0$ with the correlation length dictated by the ratio δ/γ , decreased by making γ and δ larger.

We use a uniform mesh of size 64×64 , and piecewise linear finite elements for the parameter discretization, leading to the input dimension, $d_M = 4,225$. We use a pointwise observation operator on the state at locations $\{\mathbf{x}_i \in \Omega\}_{i=1}^{50}$ so that $d_Q = 50$. Such problems are of particular relevance to Bayesian inverse problems and Bayesian optimal experimental design problems. We consider three PDE problems as follows.

3.1.1. Poisson Problem. For the first test case, we consider a lognormal diffusion (Poisson) problem in $\Omega = (0, 1)^2$ with a lognormal diffusion coefficient field $m \sim \mathcal{N}(0, \mathcal{C})$. We take $\delta = 0.5, \gamma = 0.1$ in (3.1). The observable $q(m)$ represents the observation of the PDE state $u(\mathbf{x}_i)$ on a grid in the lower half of the domain (see Figure 2). The example is taken from the `hIPPYlib` tutorial [36], the only difference is that in the tutorial the observations are random instead of grid-conforming.

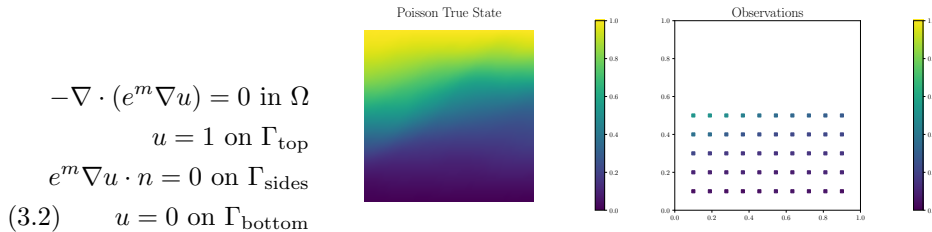


Fig. 2: An instance of Poisson state and observables

3.1.2. Reaction-Diffusion Problem. For the second test case, we consider a nonlinear reaction-diffusion problem similar to the Poisson problem state above. In this PDE formulation the right handside forcing term, \mathbf{f} , involves 25 point sources located on a Cartesian grid in the center of Ω , and additionally there is a cubic nonlinearity in the reaction term. We take $\delta = 1.0, \gamma = 0.1$. In this case there is less variance in the prior distribution, but more sensitivity to the diffusion operator due to the forcing terms and the cubic nonlinearity.

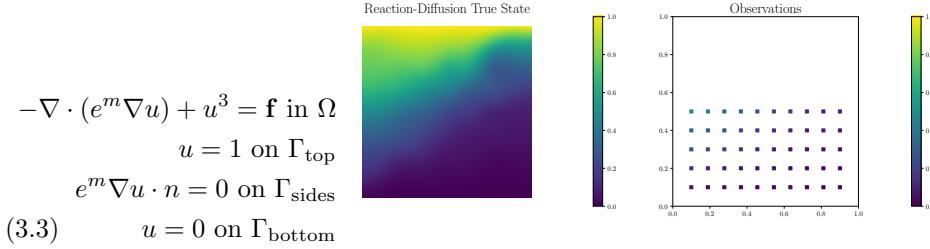


Fig. 3: An instance of reaction-diffusion state and observables

3.1.3. Convection-Reaction-Diffusion Problem. The third test case is a convection-reaction-diffusion (CRD) problem where the parameter shows up in a nonlinear reaction term[34, 39]. In this case the parameters for the distribution are $\delta = 1.0$, $\gamma = 0.1$. The quantity of interest is again a grid of observations of the PDE solution $u(\mathbf{x}_i)$ in the lower half of the domain (see Figure 4). The right hand side of the PDE is given by a Gaussian bump centered at $(0.7, 0.7)$, and the velocity field \mathbf{v} is given by a solution to a steady-state Navier-Stokes equation with walls driving the flow, for more information see the Appendices of [34].

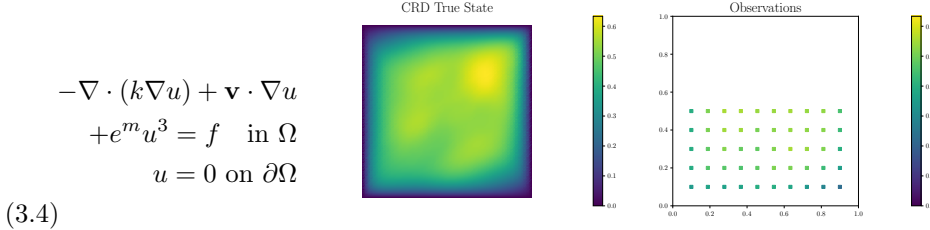


Fig. 4: An instance of CRD state and observables

3.2. Overview of Training and Accuracy Metrics. We consider three different networks architectures, one generic encoder-decoder network which we label “Generic” and then two different derivative-informed projected networks (DIPNets)[34], one with an input reduced basis dimension of $\mathbf{r}_M = 50$, and the other with a reduced basis dimension of $\mathbf{r}_M = 100$; we refer to these networks as “DIPNet 50-50” and “DIPNet 100-50” respectively as they both have full $\mathbf{r}_Q = 50$ dimensional output reduced basis representation. All three networks have six hidden layers (with latent dimension 50), and use softplus activation functions. The trainable weight dimensions are $d_W = 20,400$ for DIPNet 50-50, $d_W = 30,450$ for DIPNet 100-50, and $d_W = 226,600$ for Generic. These three networks together demonstrate the main effects that architecture can have on the quality of the approximation put forth in this work.

For each network we consider four different formulations of the loss function. The first is generic L^2 training where no derivative information is included, the second is full H^1 parametric regression where the entire H^1 semi-norm loss term is trained with equal weighting to the L^2 loss (emphasizing again in the case of DIPNet training the online costs of evaluating the H^1 semi-norm are reduced to $O(\mathbf{r}_Q \mathbf{r}_M)$). The third formulation is the reduced H^1 parametric regression problem where the reduced H^1 semi-norm term is supplemented for the entire H^1 Jacobian semi-norm, the

fourth is the same but using matrix subsampling of the Jacobian with dependent row and column samples, as in Proposition 2.2 which we denoted ‘‘MS’’. Due to limited space we do not include results for the nullspace sketching and full Jacobian sketching delineated in Section 2.2 as they performed worse than the aforementioned four approaches.

$$(3.5a) \quad L^2 : \min_w \mathbb{E}_\nu \left[\|q - f_w\|_{\ell^2(\mathbb{R}^{d_Q})} \right]$$

$$(3.5b) \quad H^1 : \min_w \mathbb{E}_\nu \left[\|q - f_w\|_{\ell^2(\mathbb{R}^{d_Q})} + \|\nabla q - \nabla f_w\|_{F(\mathbb{R}^{d_Q \times d_M})} \right]$$

(3.5c)

$$\text{Reduced } H^1 : \min_w \mathbb{E}_\nu \left[\|q - f_w\|_{\ell^2(\mathbb{R}^{d_Q})} + \|U_r^T(\nabla q - \nabla f_w)V_r\|_{F(\mathbb{R}^{r \times r})} \right]$$

(3.5d)

$$\text{Reduced } H^1\text{MS} : \min_w \mathbb{E}_\nu \left[\|q - f_w\|_{\ell^2(\mathbb{R}^{d_Q})} + \mathbb{E}_{[\hat{k}] \sim \kappa} \left[\|U_k^T(\nabla q - \nabla f_w)V_k\|_{F(\mathbb{R}^{k \times k})} \right] \right]$$

(3.5e)

We train for 100 epochs using an Adam optimizer [26], with `tensorflow`[?] default hyperparameters ($\alpha = 10^{-3}$ and 32 batch size) for simplicity. For each problem we consider training up to 4,096 data, and use 1,024 data for generalization tests. We employ three different generalization metrics: L^2 accuracy, H^1 semi-norm accuracy, and reduced H^1 semi-norm accuracy as below. The discrepancy between the H^1 semi-norm accuracy and the reduced H^1 semi-norm accuracy indicates issues with resolving the nullspace of the Jacobian over parameter space.

(3.6a)

$$L^2 \text{accuracy: } \left(1 - \mathbb{E}_\nu \left[\frac{\|q - f_w\|_{\ell^2(\mathbb{R}^{d_Q})}}{\|q\|_{\ell^2(\mathbb{R}^{d_Q})}} \right] \right)$$

(3.6b)

$$H^1 \text{ semi-norm accuracy: } \left(1 - \mathbb{E}_\nu \left[\frac{\|\nabla q - \nabla f_w\|_{F(\mathbb{R}^{d_Q \times d_M})}}{\|\nabla q\|_{F(\mathbb{R}^{d_Q \times d_M})}} \right] \right)$$

(3.6c)

$$\text{Reduced } H^1 \text{ semi-norm accuracy: } \left(1 - \mathbb{E}_\nu \left[\frac{\|\Sigma_r - U_r^T \nabla_m f_w V_r\|_{F(\mathbb{R}^{r \times r})}}{\|\Sigma_r\|_{F(\mathbb{R}^{r \times r})}} \right] \right).$$

We begin by examining the effects of derivative information on the L^2 accuracy, e.g. the approximation accuracy of the parametric map. Overall the inclusion of the derivative information in the training improved the L^2 accuracy when the number of training data is limited as shown in Figures ?? and 6. The addition of derivative information improved the accuracy of the DIPNet 100-50 significantly, in particular the matrix subsampled reduced H^1 loss function significantly improved the L^2 accuracies for limited data. The generic encoder-decoder also benefitted from additional derivative information. The results are similar for the DIPNet 50-50 network.

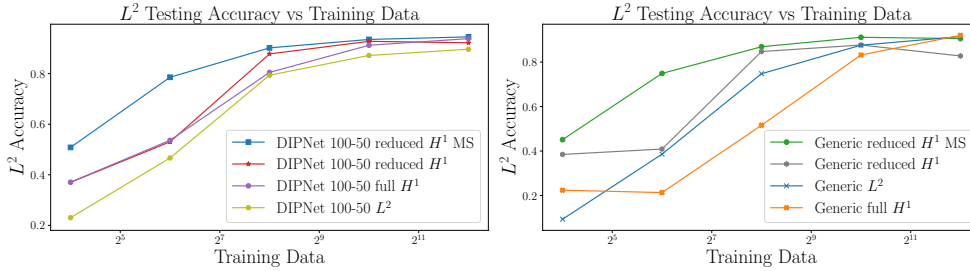


Fig. 5: Poisson L^2 training effects for the DIPNet 100-50 and Generic encoder-decoder for the four different training formulations.

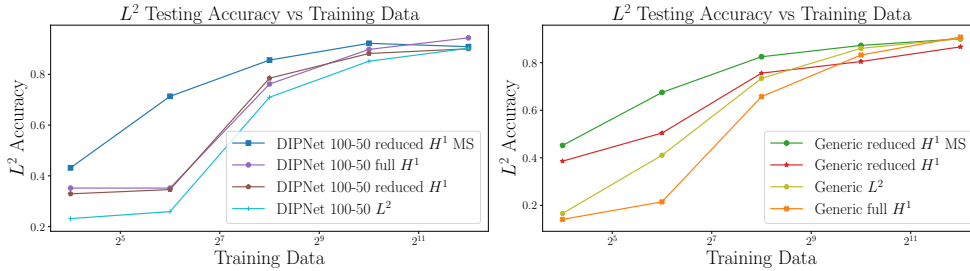


Fig. 6: Reaction-Diffusion L^2 training effects for the DIPNet 100-50 and Generic encoder-decoder for the four different training formulations.

Figure 7 demonstrates the the CRD parametric map was easier to learn than the Poisson and reaction-diffusion maps. In both cases for this easier problem the plain L^2 training performed the best by a small margin when the largest amounts of training data were present, but as with Figures ?? and 6 the additional derivative information improved the accuracy substantially in the limited training data regime.

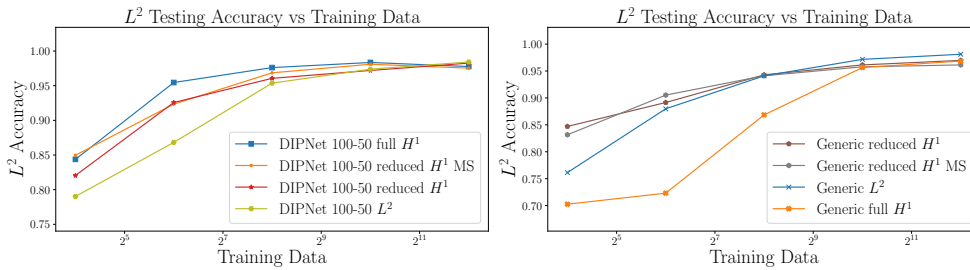


Fig. 7: Convection-Reaction-Diffusion L^2 training effects for the DIPNet 100-50 and Generic encoder-decoder for the four different training formulations.

We note that the training data axes of these plots does not make a fair comparison of computational cost for training data, since the additional Jacobian information requires extra computation. For high-dimensional nonlinear problems however, the

additional (linear) derivative information can be made very marginal relative to the cost of evaluating the nonlinear forward map $m \mapsto q$, for a discussion on this see Appendix A of [34]. Taking this into account these results make a strong case for the inclusion of derivative information in L^2 regression problems as an economical means of improving approximation accuracy for highly nonlinear problems where Jacobian matrix-products are inexpensive in comparison to the evaluation of $m \mapsto q$. In particular the matrix-subsampled reduced SVD loss was highly effective in improving parametric map accuracies.

We proceed by investigating the accuracy of the Jacobian predictions for the various architectural and optimization strategies. Starting with the Poisson and reaction-diffusion problem again, Figures 8 and 9 demonstrate that learning the entire Jacobian over parameter space is quite difficult: for these problems the best overall strategy was the DIPNet 100-50 with the full H^1 objective, and it was still only able to achieve 42.1%, 41.5% accuracy in the Poisson and reaction-diffusion problems, respectively. It is worth emphasizing that this is an extremely difficult metric to satisfy, since it requires that $d_Q \times d_M = 211, 250$ entries of the Jacobian matrix to agree for every point $m \sim \nu$. Figures 8 and 9 demonstrate that networks not trained using Jacobian information give poor approximation of Jacobian information; only the DIPNets trained with the L^2 loss gave Jacobian predictions that were better than 0% in some regime (i.e. better than the zero map). In no case was the generic L^2 network capable of producing reasonable full Jacobian predictions.

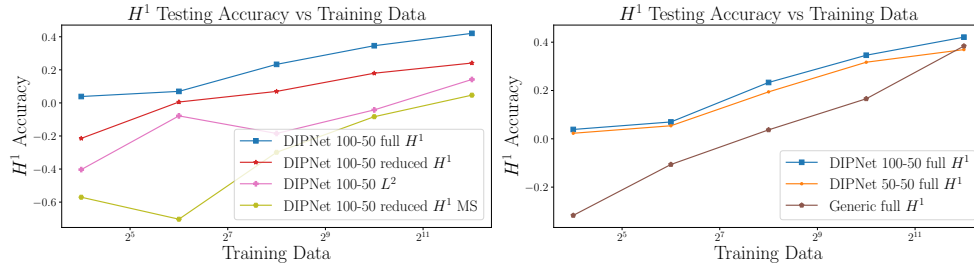


Fig. 8: Comparison of H^1 semi-norm accuracies for the Poisson problem.

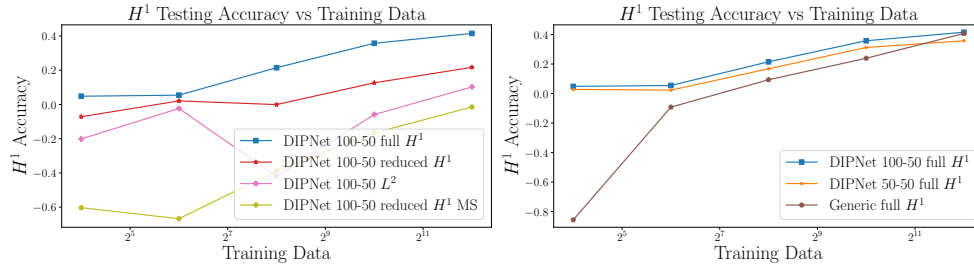


Fig. 9: Comparison of H^1 semi-norm accuracies for the reaction-diffusion problem.

As with the L^2 accuracy results, Figure 10 demonstrates that the convection-reaction-diffusion parametric Jacobian map was easier to learn than the Poisson and

reaction-diffusion problems. Figure 10 demonstrates that significantly better accuracy was achievable for the parametric Jacobian (74.7% with the full H^1 trained DIPNet 100-50 given 4,096 data). As with the previous results the only L^2 trained networks that gave greater than 0% accuracy were the DIPNets; we conjecture this is due to the derivative reduced basis construction discussed in Section 2.3.

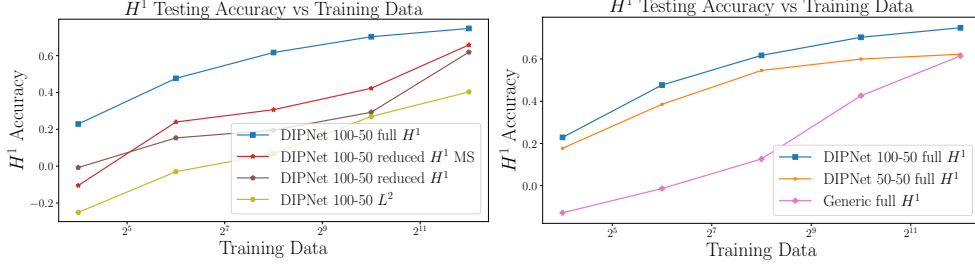


Fig. 10: Comparison of H^1 semi-norm accuracies for the convection-reaction-diffusion problem.

Figures 11, 12 and 13 demonstrate the accuracy of the Jacobian predictions in the *informed* directions of the Jacobian. The discrepancies in their performance between the H^1 and reduced H^1 accuracies is due to the effects of the reduced H^1 objective function on the nullspaces of the Jacobian. As one might expect, for this less aggressive metric the reduced H^1 metrics produced superior accuracies. In this case the DIPNet 100-50 network again produced the best overall results, in particular with the reduced H^1 optimization losses (with and without matrix sketching). These figures demonstrate that remarkably high reduced Jacobian accuracy can be achieved using the reduced H^1 objective functions, however in the case of the generic encoder-decoder, this did not lead to good overall approximation of the Jacobian. In all of these cases the accuracies have not plateaued as in the L^2 accuracy plots, which suggests that superior accuracy may be attained given more training data, and with more sophisticated optimization algorithms.

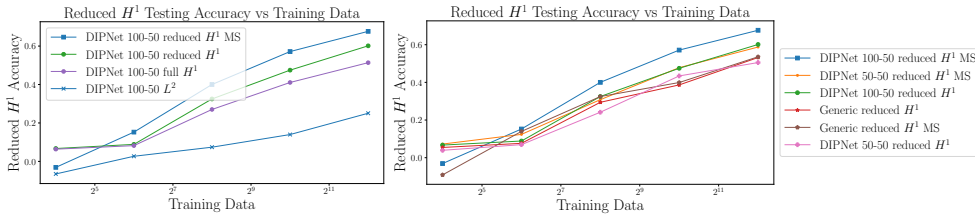


Fig. 11: Comparison of reduced H^1 semi-norm accuracies for the Poisson problem.

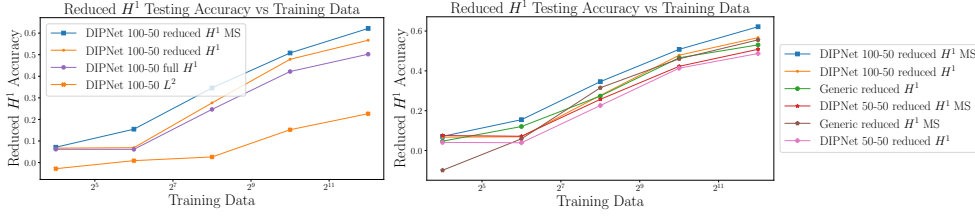


Fig. 12: Comparison of reduced H^1 semi-norm accuracies for the reaction-diffusion problem.

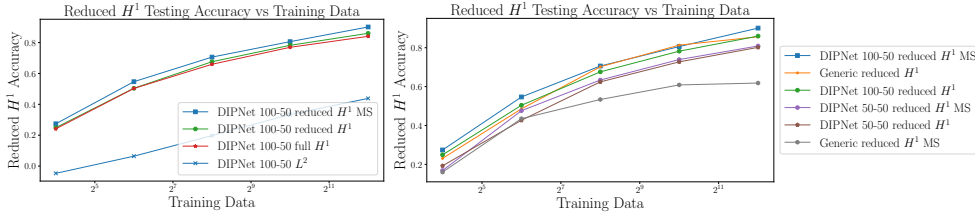


Fig. 13: Comparison of reduced H^1 semi-norm accuracies for the convection-reaction-diffusion problem.

Overall these results support the use of DIPNet reduced basis architectures for simultaneously learning the parametric map and its Jacobian. The computational complexity of this approach is significantly lower than the full H^1 learning via use of generic encoder-decoder architectures. Additionally numerical results demonstrate that this strategy led to more accurate networks in addition to being more efficient. The reduced H^1 optimization formulations did not generally lead to as good of Jacobian approximations as the full H^1 formulation, while the full H^1 formulation was less accurate in the *informed* modes of the parametric Jacobian as those trained using the reduced loss. The combination of these two approaches may lead to a better overall strategy.

4. Conclusion. To the best of our knowledge, at present neural operators aim at, and are only capable of learning parametric maps themselves, and not their derivatives. In this work we present several efficient strategies for incorporating formally high-dimensional Jacobian information, by leveraging dimension reduction techniques. When Jacobian has low rank r the offline costs of generating training data only require $O(r)$ linear Jacobian matrix-vector products, and by our proposed methods, the inclusion of this information in neural operator training need only require $O(r^2)$ memory and compute, instead of $O(d_Q d_M)$. This is achieved by making use of reduced SVD representations of the Jacobian, matrix-sketching and ultimately reduced basis architectures for neural operators that exploit derivative sensitivities of the map. We term neural operators trained using these frameworks derivative informed neural operators (DINOs).

Numerical results demonstrate that the inclusion of derivative information in the optimization problem leads to superior approximation of the parametric map, especially when only limited training data are available, in particular by using the

highly efficient reduced H^1 optimization formulation. This is an important point, as it demonstrates that additional derivative information can be supplemented for parametric map evaluations to improve the accuracy of the training, when only few training data are available. This is useful for highly nonlinear maps where the costs of (linear) derivatives are marginal in relation to the cost of the nonlinear map itself.

Additionally, numerical results demonstrate that the high-dimensional parametric Jacobian is hard to learn to typical accuracy requirements using neural operators. Our results show that the Jacobian accuracy from simple L^2 training was poor, and the inclusion of derivative information in the training significantly improved the Jacobian approximations. The best strategies for learning the parametric Jacobian accurately, was by imposing the full Jacobian error loss. This strategy worked well for all the networks we investigated, however as was discussed in Section 2.3, this strategy is only scalable by making use of reduced-basis architecture, in particular, DIPNets; in this case the computational complexity of learning the full Jacobian is reduced from $O(d_Q d_M)$ to $O(r^2)$, where r is the dimension of the reduced bases.

The reduced H^1 strategies that we proposed are generally efficient independent of the neural operator's architecture, but gave mixed results in Jacobian accuracy. We note that this may be a more suitable metric for the reliable deployment of these networks in derivative based inference methods. In ongoing experiments we have observed that DINOs with good reduced H^1 approximations but less accurate H^1 approximations as in Figures 8 - 10 were able to provide accurate computations used in Bayesian inverse problems, where the prior information plays a dominant role in the nullspaces. This will be further explored in an upcoming paper.

In this work the multi-objective optimization formulation was equally weighted, and made use of simple optimization algorithms. In future work we expect the performance of the models could be improved by the use of Pareto fronts and more sophisticated optimization routines.

All in all DINO provides a framework for scalably incorporating derivative information into the training of neural operators. This not only improves parametric map approximations when only limited training data are available, but also provides a path to the deployment of DINOs in outer-loop algorithms that make use of parametric derivative information.

REFERENCES

- [1] A. ALEXANDERIAN, N. PETRA, G. STADLER, AND O. GHATTAS, *A fast and scalable method for A-optimal design of experiments for infinite-dimensional Bayesian nonlinear inverse problems*, SIAM Journal on Scientific Computing, 38 (2016), pp. A243–A272, <https://doi.org/10.1137/140992564>.
- [2] A. ALEXANDERIAN, N. PETRA, G. STADLER, AND O. GHATTAS, *Mean-variance risk-averse optimal control of systems governed by PDEs with random parameter fields using quadratic approximations*, SIAM/ASA Journal on Uncertainty Quantification, 5 (2017), pp. 1166–1192, <https://doi.org/10.1137/16M106306X>. arXiv preprint arXiv:1602.07592.
- [3] N. ALGER, P. CHEN, AND O. GHATTAS, *Tensor train construction from tensor actions, with application to compression of large high order derivative tensors*, SIAM Journal on Scientific Computing, 42 (2020), pp. A3516–A3539.
- [4] O. BASHIR, K. WILLCOX, O. GHATTAS, B. VAN BLOEMEN WAANDERS, AND J. HILL, *Hessian-based model reduction for large-scale systems with initial condition inputs*, International Journal for Numerical Methods in Engineering, 73 (2008), pp. 844–868.
- [5] A. BESKOS, M. GIROLAMI, S. LAN, P. E. FARRELL, AND A. M. STUART, *Geometric MCMC for infinite-dimensional inverse problems*, Journal of Computational Physics, 335 (2017), pp. 327–351.
- [6] K. BHATTACHARYA, B. HOSSEINI, N. B. KOVACHKI, AND A. M. STUART, *Model reduction and*

neural networks for parametric PDEs, arXiv preprint arXiv:2005.03180, (2020).

[7] D. BIGONI, Y. MARZOUK, C. PRIEUR, AND O. ZAHM, *Nonlinear dimension reduction for surrogate modeling using gradient information*, arXiv preprint arXiv:2102.10351, (2021).

[8] M. BRENNAN, D. BIGONI, O. ZAHM, A. SPANTINI, AND Y. MARZOUK, *Greedy inference with structure-exploiting lazy maps*, Advances in Neural Information Processing Systems, 33 (2020).

[9] T. BUI-THANH, C. BURSTEDDE, O. GHATTAS, J. MARTIN, G. STADLER, AND L. C. WILCOX, *Extreme-scale UQ for Bayesian inverse problems governed by PDEs*, in SC12: Proceedings of the International Conference for High Performance Computing, Networking, Storage and Analysis, 2012.

[10] T. BUI-THANH AND O. GHATTAS, *An analysis of infinite dimensional Bayesian inverse shape acoustic scattering and its numerical approximation*, SIAM/ASA Journal of Uncertainty Quantification, 2 (2014), pp. 203–222, <https://doi.org/http://dx.doi.org/10.1137/120894877>.

[11] T. BUI-THANH, O. GHATTAS, J. MARTIN, AND G. STADLER, *A computational framework for infinite-dimensional Bayesian inverse problems Part I: The linearized case, with application to global seismic inversion*, SIAM Journal on Scientific Computing, 35 (2013), pp. A2494–A2523, <https://doi.org/10.1137/12089586X>.

[12] P. CHEN AND O. GHATTAS, *Hessian-based sampling for high-dimensional model reduction*, International Journal for Uncertainty Quantification, 9 (2019).

[13] P. CHEN AND O. GHATTAS, *Projected Stein variational gradient descent*, in Advances in Neural Information Processing Systems, 2020.

[14] P. CHEN, M. HABERMAN, AND O. GHATTAS, *Optimal design of acoustic metamaterial cloaks under uncertainty*, Journal of Computational Physics, 431 (2021), p. 110114.

[15] P. CHEN, U. VILLA, AND O. GHATTAS, *Hessian-based adaptive sparse quadrature for infinite-dimensional Bayesian inverse problems*, Computer Methods in Applied Mechanics and Engineering, 327 (2017), pp. 147–172, <https://doi.org/10.1016/j.cma.2017.08.016>.

[16] P. CHEN, U. VILLA, AND O. GHATTAS, *Taylor approximation and variance reduction for PDE-constrained optimal control under uncertainty*, Journal of Computational Physics, 385 (2019), pp. 163–186, <https://arxiv.org/abs/1804.04301>.

[17] P. CHEN, K. WU, J. CHEN, T. O'LEARY-ROSEBERRY, AND O. GHATTAS, *Projected Stein variational Newton: A fast and scalable Bayesian inference method in high dimensions*, Advances in Neural Information Processing Systems, (2019).

[18] P. G. CONSTANTINE, E. DOW, AND Q. WANG, *Active subspace methods in theory and practice: applications to kriging surfaces*, SIAM Journal on Scientific Computing, 36 (2014), pp. A1500–A1524.

[19] B. CRESTEL, A. ALEXANDERIAN, G. STADLER, AND O. GHATTAS, *A-optimal encoding weights for nonlinear inverse problems, with application to the Helmholtz inverse problem*, Inverse Problems, 33 (2017), p. 074008, <http://iopscience.iop.org/10.1088/1361-6420/aa6d8e>.

[20] T. CUI, K. LAW, AND Y. MARZOUK, *Dimension-independent likelihood-informed MCMC*, Journal of Computational Physics, 304 (2016), pp. 109–137.

[21] W. M. CZARNECKI, S. OSINDERO, M. JADERBERG, G. SWIRSZCZ, AND R. PASCANU, *Sobolev training for neural networks*, Advances in Neural Information Processing Systems, 30 (2017).

[22] P. H. FLATH, L. C. WILCOX, V. AKÇELIK, J. HILL, B. VAN BLOEMEN WAANDERS, AND O. GHATTAS, *Fast algorithms for Bayesian uncertainty quantification in large-scale linear inverse problems based on low-rank partial Hessian approximations*, SIAM Journal on Scientific Computing, 33 (2011), pp. 407–432, <https://doi.org/10.1137/090780717>.

[23] S. FRESCA AND A. MANZONI, *Pod-dl-rom: enhancing deep learning-based reduced order models for nonlinear parametrized pdes by proper orthogonal decomposition*, Computer Methods in Applied Mechanics and Engineering, 388 (2022), p. 114181.

[24] N. HALKO, P.-G. MARTINSSON, AND J. A. TROPP, *Finding structure with randomness: Probabilistic algorithms for constructing approximate matrix decompositions*, SIAM review, 53 (2011), pp. 217–288.

[25] T. ISAAC, N. PETRA, G. STADLER, AND O. GHATTAS, *Scalable and efficient algorithms for the propagation of uncertainty from data through inference to prediction for large-scale problems, with application to flow of the Antarctic ice sheet*, Journal of Computational Physics, 296 (2015), pp. 348–368, <https://doi.org/10.1016/j.jcp.2015.04.047>.

[26] D. P. KINGMA AND J. BA, *Adam: A method for stochastic optimization*, arXiv preprint arXiv:1412.6980, (2014).

[27] N. KOVACHKI, Z. LI, B. LIU, K. AZIZZADEHESHELI, K. BHATTACHARYA, A. STUART, AND A. ANANDKUMAR, *Neural operator: Learning maps between function spaces*, arXiv pre-

print arXiv:2108.08481, (2021).

[28] Z. LI, N. KOVACHKI, K. AZIZZADENESHELI, B. LIU, K. BHATTACHARYA, A. STUART, AND A. ANANDKUMAR, *Fourier neural operator for parametric partial differential equations*, arXiv preprint arXiv:2010.08895, (2020).

[29] Z. LI, N. KOVACHKI, K. AZIZZADENESHELI, B. LIU, K. BHATTACHARYA, A. STUART, AND A. ANANDKUMAR, *Neural operator: Graph kernel network for partial differential equations*, arXiv preprint arXiv:2003.03485, (2020).

[30] A. MANZONI, F. NEGRI, AND A. QUARTERONI, *Dimensionality reduction of parameter-dependent problems through proper orthogonal decomposition*, Annals of Mathematical Sciences and Applications, 1 (2016), pp. 341–377.

[31] P. G. MARTINSSON AND J. TROPP, *Randomized Numerical Linear Algebra: Foundations & Algorithms*, arXiv preprint arXiv:2002.01387, (2020).

[32] N. H. NELSEN AND A. M. STUART, *The random feature model for input-output maps between banach spaces*, arXiv preprint arXiv:2005.10224, (2020).

[33] T. O'LEARY-ROSEBERRY, X. DU, A. CHAUDHURI, J. R. MARTINS, K. WILLCOX, AND O. GHATTAS, *Adaptive projected residual networks for learning parametric maps from sparse data*, arXiv preprint arXiv:2112.07096, (2021).

[34] T. O'LEARY-ROSEBERRY, U. VILLA, P. CHEN, AND O. GHATTAS, *Derivative-informed projected neural networks for high-dimensional parametric maps governed by PDEs*, Computer Methods in Applied Mechanics and Engineering, 388 (2022), p. 114199.

[35] M. RAISSI, P. PERDIKARIS, AND G. E. KARNIADAKIS, *Physics-informed neural networks: A deep learning framework for solving forward and inverse problems involving nonlinear partial differential equations*, Journal of Computational Physics, 378 (2019), pp. 686–707.

[36] U. VILLA, N. PETRA, AND O. GHATTAS, *hIPPYlib: An Extensible Software Framework for Large-Scale Inverse Problems Governed by PDEs; Part I: Deterministic Inversion and Linearized Bayesian Inference*, Transactions on Mathematical Software, in print (2020), <https://arxiv.org/abs/1909.03948>.

[37] K. WU, P. CHEN, AND O. GHATTAS, *A fast and scalable computational framework for large-scale and high-dimensional Bayesian optimal experimental design*, arXiv preprint arXiv:2010.15196, (2020).

[38] K. WU, P. CHEN, AND O. GHATTAS, *An efficient method for goal-oriented linear bayesian optimal experimental design: Application to optimal sensor placement*, arXiv preprint arXiv:2102.06627, (2021).

[39] K. WU, T. O'LEARY-ROSEBERRY, P. CHEN, AND O. GHATTAS, *Derivative-informed projected neural network for large-scale Bayesian optimal experimental design*, arXiv preprint arXiv:2201.07925, (2022).

[40] J. YU, L. LU, X. MENG, AND G. E. KARNIADAKIS, *Gradient-enhanced physics-informed neural networks for forward and inverse pde problems*, Computer Methods in Applied Mechanics and Engineering, 393 (2022), p. 114823.

[41] O. ZAHM, P. G. CONSTANTINE, C. PRIEUR, AND Y. M. MARZOUK, *Gradient-based dimension reduction of multivariate vector-valued functions*, SIAM Journal on Scientific Computing, 42 (2020), pp. A534–A558.

[42] O. ZAHM, T. CUI, K. LAW, A. SPANTINI, AND Y. MARZOUK, *Certified dimension reduction in nonlinear Bayesian inverse problems*, arXiv preprint arXiv:1807.03712, (2018).